

TOWARDS WALL-ADAPTION OF TURBULENCE MODELS WITHIN THE LATTICE BOLTZMANN FRAMEWORK

Patrick Nathen

Institute for Aerodynamics and Fluid Mechanics
 Technische Universität München
 Boltzmannstr. 15, 85748 Garching bei München, Germany
 patrick.nathen@aer.mw.tum.de

Daniel Gaudlitz¹ and Nikolaus Adams²

Institute for Aerodynamics and Fluid Mechanics
 Technische Universität München
 Boltzmannstr. 15, 85748 Garching bei München, Germany

ABSTRACT

This paper presents the development towards wall adaptive explicit filters for the simulation of turbulent wall bounded flows in the framework of the lattice Boltzmann method (LBM). First, we show the effect of different collision models on the characteristics of turbulent flow simulations by employing the Taylor-Green vortex as a numerical testcase. Second, an extension of the approximate deconvolution method (ADM), see Malaspinas & Sagaut (2012), Malaspinas & Sagaut (2011) and Sagaut (2010) for the simulation of wall-bounded turbulent flows is presented. A temporal dissipation relaxation is applied for explicit filtering, in order to suppress filtering in regions, where the flow is resolved and to adapt filtering in underresolved regions in such way, that the energy drain in the scales is physically motivated and consistent with the kinetic theory of turbulence. We apply the extended ADM for the simulation of a turbulent channel flow at $Re_\tau = 180$ and $Re_\tau = 395$ to demonstrate, that the ADM method of Malaspinas & Sagaut (2011) with selective viscosity filters is strictly dissipative for low-order filters. Hence, especially for wall-bounded flows the application of the proposed adaptive relaxation of the filter can be beneficial.

The lattice-Boltzmann method

LBM solves a set of kinetic equations in terms of discrete velocity distribution functions $f_\alpha(t, \mathbf{x})$ numerically. The discrete Boltzmann equations can be written as

$$f_\alpha(t + \Delta t, \mathbf{x} + \mathbf{c}_\alpha \Delta t) = f_\alpha(t, \mathbf{x}) + \Omega_\alpha(f_\alpha(t, \mathbf{x})) \quad (1)$$

where $\Omega_\alpha(f_\alpha(t, \mathbf{x}))$ is the collision operator, which represents non-linear and viscous effects of the Navier Stokes equations and \mathbf{c}_α is the discrete velocity set of the lattice applied. Macroscopic moments are reconstructed with a Gauss-Hermite quadrature based on the Hermite Polynomial expansion on a discrete lattice. The first two moments

of the velocity distribution functions are the conserved moments ρ and the momentum $\rho \mathbf{u}$, which read

$$\rho = \sum_\alpha f_\alpha, \quad \rho \mathbf{u} = \sum_\alpha \mathbf{c}_\alpha f_\alpha \quad (2)$$

while the momentum flux is the second-order off-equilibrium moment of the velocity distribution functions

$$\Pi = \sum_\alpha f_\alpha^{neq} \mathbf{c}_\alpha \mathbf{c}_\alpha \quad (3)$$

In order to reconstruct the macroscopic equations of fluid motion, a Chapman Enskog expansion is used. The interested reader can refer to Chen & Doolen (1998) among others.

To close equation (1) the collision term needs to be modeled. One well-known approach is the linearization around small perturbations of the thermodynamic equilibrium. This approach is called the Bhatnagar-Gross-Krook (BGK) ansatz, see He & Luo (1997); Guo *et al.* (2000); Guo & Shu (2013) or Sukop & Thorne (2006) among others, which represents the collision term as a linear relaxation towards a Maxwellian equilibrium

$$\begin{aligned} \Omega_\alpha(f_\alpha(t, \mathbf{x})) &= f_\alpha(t + \Delta t, \mathbf{x} + \mathbf{c}_\alpha \Delta t) - f_\alpha(t, \mathbf{x}) \\ &= -\frac{1}{\tau} (f_\alpha(t, \mathbf{x}) - f_\alpha^{eq}(t, \mathbf{x})). \end{aligned} \quad (4)$$

$f_\alpha^{eq}(t, \mathbf{x})$ is a low Mach number truncated Maxwell-Boltzmann distribution, which is adjusted in such a way, that equation (3) is fulfilled and mass and momentum are conserved. A widely used formulation for f_α^{eq} is given by

$$f_\alpha^{eq} = \rho \omega_\alpha \left[1 + \frac{\mathbf{c}_\alpha \mathbf{u}}{c_s^2} + \frac{1}{2c_s^4} (\mathbf{u} \mathbf{u} - c_s^2 \boldsymbol{\delta}) \mathbf{u} \mathbf{u} \right]. \quad (5)$$

ω_α are the weights to satisfy the exact Gauss-Hermite quadrature of the lattice, c_s is the lattice speed of sound and

¹daniel.gaudlitz@aer.mw.tum.de

²nikolaus.adams@tum.de

δ is the Kronecker delta. Although, the BGK approach has been applied to many flow problems, see Hänel (2004) and Waldrow (2000), it has been found to suffer from instabilities at high Reynolds numbers, which have its origins in unphysical moments of f_α . To remedy this shortcoming, the Multi-Relaxation-Time (MRT) scheme was developed by D'Humières *et al.* (2002). The main idea is to transform the collision step into the momentum space and to relax each moment separately in order to reduce the instabilities arising from the temporal growth of these unphysical moments. Thus, the single relaxation time from the BGK model is replaced by a relaxation time matrix \mathbf{S} , which relaxes each moment $m_\alpha = \mathbf{M}f_\alpha$ independently. The matrix \mathbf{M} is a linear transformation matrix and the corresponding algorithm for the MRT scheme reads

$$\begin{aligned} f_\alpha(t + \Delta t, \mathbf{x} + \mathbf{c}_\alpha \Delta t) - f_\alpha(t, \mathbf{x}) \\ = -\mathbf{M}^{-1} \mathbf{S} (m_\alpha(t, \mathbf{x}) - m_\alpha^{eq}(t, \mathbf{x})) \end{aligned} \quad (6)$$

The MRT model increases the stability of the LBM method substantially. Yet, e.g. due to inconsistent derivation of boundary conditions for stresses on domain boundaries, where velocities are prescribed, instabilities arise in the MRT model for Reynolds numbers larger than approx. 5000 for three dimensional flows, see Freitas *et al.* (2011). In order to suppress these exponentially growing disturbances, Latt (see Latt & Chopard (2006) and Latt (2007)) proposed a regularization of the classical BGK algorithm, employing an approximation of the first-order multiscale expansion term

$$f_\alpha^{neq} = f_\alpha - f_\alpha^{eq} \approx f_\alpha^{(1)} = -\frac{\Delta t}{\omega c_s^2} \omega_\alpha \mathbf{Q}_\alpha \partial_i \rho \mathbf{u}. \quad (7)$$

Here, \mathbf{Q}_α is the first-order non equilibrium moment $\mathbf{Q}_\alpha = \sum \mathbf{c} \mathbf{c} f_\alpha^{neq}$. The non-equilibrium distribution function f_α^{neq} is used to approximate the first-order multiscale expansion term. This term is included in the BGK model, thus the regularized BGK algorithm reads

$$f_\alpha(t + \Delta t, \mathbf{x} + \mathbf{c}_\alpha \Delta t) = f_\alpha(t, \mathbf{x}) + (1 - \omega) f_\alpha^{(1)}(t, \mathbf{x}) \quad (8)$$

This regularization operation is not only necessary for the flow field, but also for the boundaries. The main issue with respect to boundary conditions in the RLB is the proper reconstruction of the unknown distribution functions propagating into the flow domain. Since for the regularization the discrete velocity information is needed, a proper approximation of the non-equilibrium part $f_\alpha^{(1)}$ in equation (7) is required. Different approaches to model $f_\alpha^{(1)}$ at domain boundaries are proposed in Latt (2007) and Latt *et al.* (2008). In the present investigation the interpolated boundary approximation of the strain rate is considered for wall-bounded flows only.

The approximate deconvolution method (ADM) for LBM

The turbulence model investigated in this paper, which is adapted for wall-bounded flows, is the approximate deconvolution method (ADM) of Stolz & Adams (1999),

Adams & Stolz (2002) and Stolz *et al.* (2001). The concept of ADM is a generalization of the scale-similarity model for Large-Eddy simulation based subgrid-scale models. The consecutive steps of explicit filtering and subsequent deconvolution of the macroscopic equations for fluid motions was adopted by Sagaut (2010) and Malaspinas & Sagaut (2011) in the LBM framework using a selective viscosity filter, see Tam *et al.* (1993). Applying a homogeneous low-pass filter kernel G on equation (1) one receives

$$\overline{\frac{Df_\alpha(t, \mathbf{x})}{Dt}} = \overline{\Omega_\alpha(f_\alpha(t, \mathbf{x}))} \quad (9)$$

which is equal to

$$\begin{aligned} \overline{\frac{Df_\alpha(t, \mathbf{x})}{Dt}} - \Omega_\alpha(\overline{f_\alpha(t, \mathbf{x})}) \\ = G * \Omega_\alpha(f_\alpha(t, \mathbf{x})) - \Omega_\alpha(\overline{f_\alpha(t, \mathbf{x})}) = \sigma_{sgs} \end{aligned} \quad (10)$$

where σ_{sgs} is the subgrid stress term emerging from the discrepancy between exact convolution and computable terms. In general two approaches are followed at this point, which can be easily shown by re-writing the right-hand side of equation (10) as

$$\begin{aligned} [G * \Omega_\alpha(\hat{f}_\alpha(t, \mathbf{x})) - \Omega_\alpha(\overline{f_\alpha(t, \mathbf{x})})] \\ + [G * \Omega_\alpha(f_\alpha(t, \mathbf{x})) - \Omega_\alpha(\hat{f}_\alpha(t, \mathbf{x}))] \\ = \sigma_{sgs} = \sigma_{sgs}^1 + \sigma_{sgs}^2 \end{aligned} \quad (11)$$

where σ_{sgs}^1 is the known term and σ_{sgs}^2 is the unknown term which needs to be modeled and $\hat{f}_\alpha(t, \mathbf{x})$ is the approximate deconvolution of the distribution function. At this point either the term σ_{sgs}^2 is modeled as demonstrated in Sagaut (2010) and Malaspinas & Sagaut (2011), or the simplified version of Stolz, Adams and additionally Mathew Mathew *et al.* (2003), is applied where the exact distribution function is replaced by its approximate inverse $G * \Omega_\alpha(f_\alpha(t, \mathbf{x})) \approx G * \Omega_\alpha(\hat{f}_\alpha(t, \mathbf{x}))$. This simplification is valid for $f_\alpha \approx \overline{f_\alpha}$ and has a tremendous effect on the required filter properties, since the discretization scheme in LBM is fixed and thus the ADM-LES approach itself is decoupled from the filter operation in the LBM framework. In earlier work, see Pruetz & Adams (2000), the authors showed that indeed the underlying LES model cannot be chosen independently from the applied filter. Thus, if the filter operation is decoupled from our discretization scheme and the subgrid-scale model, the filter procedure can be adjusted in such way to act only on the scales intended. Using the simplified procedure, equation (11) reduces to

$$\begin{aligned} \overline{\frac{Df_\alpha(t, \mathbf{x})}{Dt}} - \Omega_\alpha(\overline{f_\alpha(t, \mathbf{x})}) \\ = G * \Omega_\alpha(\hat{f}_\alpha(t, \mathbf{x})) - \Omega_\alpha(\overline{f_\alpha(t, \mathbf{x})}) = \sigma_{sgs}^1. \end{aligned} \quad (12)$$

The simplified approach given in equation (12) is the underlying approach in the current investigation. An inverse filter operation is performed with a deconvolution operator $\hat{\phi} = G^{-1} * \overline{\phi} = Q * \overline{\phi}$. The quality of an inverse filter operation is described with the transfer function $\hat{G}(\xi)$ in spectral space, where ξ is the wavenumber. In the work of Stolz

& Adams (1999), Adams & Stolz (2002) and Stolz *et al.* (2001), a Padé filter was applied and the deconvoluted solution is obtained by the Van Cittert iterative method. The authors showed, that a high-order deconvolution can be provided up to the cut-off wavenumber of the applied filter. Sagaut (2010) and Malaspinas & Sagaut (2011) used a class of selective viscosity filters up to order $N = 4$. In Tam *et al.* (1993), the stencil properties were derived and compared to each other. These filters damp high-wavenumber parts of an arbitrary signal, employing a damping approach, which reads

$$\hat{f}_\alpha^{out}(t, \mathbf{x}) = \bar{f}_\alpha^{in}(t, \mathbf{x}) - \sigma \sum_{n=-j}^j d_n \bar{f}_\alpha^{in}(t, \mathbf{x} + \mathbf{e}_n) \quad (13)$$

where the filter strength σ is related to an artificial viscosity and d_n is the weighting coefficient. In figure 1

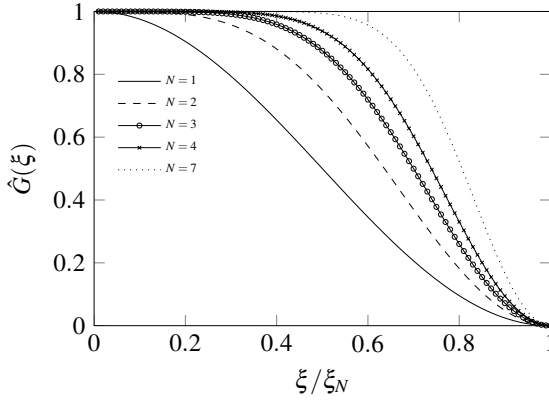


Figure 1: Transfer functions of the filters used by Malaspinas & Sagaut (2011) for the ADM $N = 1.4$ and an additional high-order viscosity filter $N = 7$ from Tam *et al.* (1993). The wavenumber is normalized with the Nyquist wavenumber ξ_N

the filters used for ADM by Malaspinas & Sagaut (2011) are shown in terms of the transfer function. It is visible, that even for the highest orders of the viscosity filters, the damping is quite strong. Hence, the underlying assumption $\hat{f}_\alpha \approx \bar{f}_\alpha$ for applying an explicit filter shown in figure 1 in the framework of the simplified procedure is questionable. A very high filter stencil is necessary in order to be consistent with the underlying assumptions made in this context. This is not desirable for the LBM, since its algorithm is executed locally and any non-local operation drains the computational efficiency dramatically. Especially, if one considers an inverse convolution of each discrete lattice velocity would render the LBM algorithm inappropriate for flow problems.

From a computational point of view, we focus on the deconvolution of the macroscopic moments and aim to modify the strength of the filter σ as a function of space and time $\sigma(\mathbf{x}, t)$ instead of leaving it constant. Thus, we cannot increase the order, and subsequently the steepness of the transferfunction, but the scales on which the filter operation will be applied. Therefore we aim to develop a selective

viscosity filter, where the filter strength is adjusted in such way, that even low filter orders operate on large wavenumber only scales and thus $\hat{f}_\alpha \approx \bar{f}_\alpha$ is satisfied. With this approach, filtering is adopted to the mesh resolution automatically in terms of the resolved scales.

Our approach is based on the idea of the shear-improved Smagorinsky model of Lèveque *et al.* (2007). This model is based on the idea, that resolved turbulent scales in terms of the resolved strain-rate relax towards an average strain-rate and thus the fluctuating part of the strain-rate is significant at scales of filter size Δ_x . In flow regions, where the fluctuating part of the strain-rate is larger than the average strain rate, the turbulent flow can be considered as homogeneous and the standard Smagorinsky model is reconstructed. This approach was adopted earlier by Jafari & Rahnama (2011) for the MRT-based lattice Boltzmann, but the application was only limited to low Reynolds numbers. Also as shown by Malaspinas & Sagaut (2012), the modification of the effective relaxation rate does not inevitably lead to the filtered equations of fluid motions, namely the filtered Navier-Stokes equations. We apply a relaxation of the filter strength in terms of the temporal averaged resolved strain-rate. Without loss of generalization, a temporal averaging procedure is used since in statistically steady flows, like the converged turbulent channel flow, the efficiency increases (local operation), the spatial averaged statistics are reconstructed as well (ergodic system) and it is also suitable for the application to complex flows, with arbitrary flow separations. The filter strength is computed as

$$\sigma(t, \mathbf{x}) = \frac{(|S|_{ij}(t, \mathbf{x}) - \langle |S|_{ij}(\mathbf{x}) \rangle) \Delta_t v}{(\rho + \langle \delta \rho \rangle)} \frac{1}{2} \left(\frac{\omega}{c_s^2} \right)^2 \quad (14)$$

where $\langle |S|_{ij} \rangle$ is the time averaged resolved strain-rate and Δ_t the physical time step. Averaging is performed as soon as the flows achieves a statistically steady state in terms of an autocorrelation function.

$$\eta = \frac{\langle u_x(\mathbf{x}, t) u_x(\mathbf{x}, t + \tau) \rangle}{\langle u_x(\mathbf{x}, t) u_x(\mathbf{x}, t) \rangle} \quad (15)$$

For flows with strong unsteady effects as they appear in external aerodynamics, a phase-averaging procedure is the straight forward extension of this adaptive explicit filtering step. Despite the fact, that a time correlation needs to be estimated, the computational costs are very low compared with other approaches like the dynamic Smagorinsky model. Although we have a non-local filter approach, which reduces the computational efficiency, this approach is consistent with the macroscopic limit of the filtered equations of fluid motion. The filter-subgrid-scale model coupling and no loss of generalization in terms of Reynolds number and mesh requirements is present.

Beyond this, any amplification of unphysical moments are suppressed, since non-physical strain rates are only locally apparent and damped by our temporal adapted explicit filtering step. It is worth to mention, that the amplification of unphysical moments in terms of the strain-rate lead to an overpredicted eddy-viscosity for standard approaches in the LBM framework since the strain-rate and thus the non-equilibrium part of the velocity distribution function is directly linked to the turbulent relaxation time. This is a promising step towards BGK based simulation for high

Reynolds number flows where the stabilization is consistent with a physically motivated energy drain.

Analysis of the discrete lattice schemes for the simulation of turbulent flows

In order to investigate the properties of the different collision models, we employ the well-known Taylor-Green vortex and analyze the intergral dissipation rate. It will be outlined, why the BGK collision model is our model of choice. Prior analysis showed, that the BGK and MRT model have a oppositioned behavior: While the BGK scheme tends to be unstable if the Reynolds number is increased at a fixed mesh resolution, the MRT scheme showed no mesh convergence at a fixed mach number if the mesh resolution is increased at a fixed Reynolds number. This is exemplified for the Reynolds number $Re = 3000$ and two different mesh resolutions, $N = 64$ and $N = 256$, in figure 2.

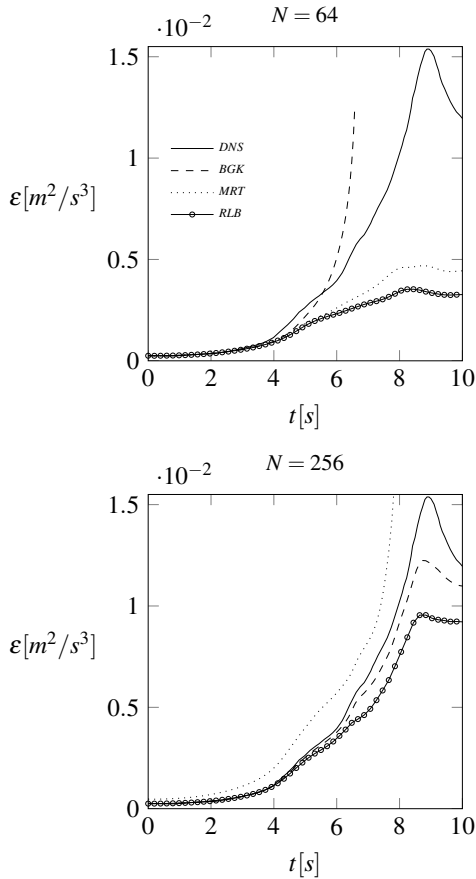


Figure 2: Temporal evolution of the dissipation rate of the Taylor-Green vortex predicted by the BGK, MRT and RLB scheme at $Re = 3000$ for the resolutions $N = 64$ and 256 .

While the BGK scheme diverged for the lowest resolution which corresponds to the findings of others, see Lallemand & Luo (2000) and He & Luo (1997), the MRT

scheme showed no convergence if the mesh resolution was increased to $N = 256$.

Beyond this, it was found that the RLB collision model is unconditionally stable at all resolutions and Reynolds numbers, but it suffers from a rather strong additional numerical viscosity. In order to represent the same range of turbulent scales for a given Reynolds number with the RLB scheme, additional computational effort has to be taken into account in terms of an increased resolution.

Based on these investigations, the BGK collision model was chosen for all further investigations, since mesh convergence was proven and the instabilities at high Reynolds numbers and low resolutions can be damped by our new model.

The turbulent channel flow

The aim of this work is to provide an extension of the ADM in the framework of the LBM. The model should adapt automatically the filtering strength to the local resolved scales. In regions where turbulence is resolved, filtering is suppressed by an energy drain balance, while in regions where the flow is underresolved, explicit filtering is adapted in such way, that the energy drain caused by filtering corresponds to a physically motivated viscosity model. The test case chosen is based on the work of Bepalko (2011). The domain had the extensions of $L_x = 12H$, $L_y = 4H$ and $L_z = 2H$ for the streamwise, lateral and wall normal direction respectively, where H is the channel half width. In streamwise and lateral direction, periodic boundary conditions were applied. Constant forcing in streamwise direction was applied as in Bepalko (2011). At the bottom and the top of the domain a halfway bounce-back rule, combined with a non-linear finite-difference regularization was applied, see Latt *et al.* (2008). In order to investigate the general sensitivity of the ADM for wall-bounded flows, we first apply the ADM with different filter stencils ($2nd$ and $3rd$ order) and filter strengths ($\sigma = 0.001$ and $\sigma = 0.005$) to the turbulent channel flow at $Re_\tau = 180$. This is the smallest Reynolds numbers for turbulent scales in a turbulent channel flow. DNS reference data is taken from Kim *et al.* (1987) and Moser *et al.* (1999). In figure 3 the influence of the pure filtering on the turbulent velocity field is shown.

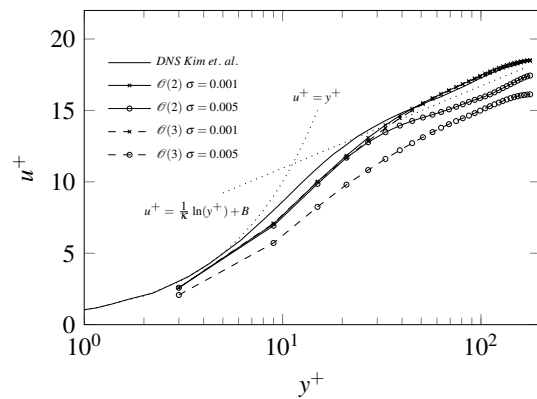


Figure 3: Mean velocity profiles of turbulent channel flow at $Re_\tau = 180$. Comparison of reference DNS of Kim *et al.* (1987) to the underresolved simulations with the BGK-based ADM model.

As it is clearly recognizable, the influence of the order of the filter is inferior to the applied filter strength, since the difference in the predicted velocity profiles by the BGK-based ADM is rather small for the lower filter strength compared with the DNS data. For the higher filter strength both filters underpredict velocity field, especially in the log-region of the flow. In previous investigations, it has been shown that the BGK model without any turbulence model has a good agreement with the DNS data for $y^+ < 30$, but in the bulk regions the average flow field was overpredicted. In the current study, the influence of explicit filtering leads a "shift-down" of the average velocity field, which indicates the necessity of selective filtering. This "shift-down" is also marginally influenced by the constant forcing as shown later.

The proposed model should filter mainly in the bulk region, while the wall-nearest region should be unaffected by the filtering procedure. The Reynolds numbers $Re_\tau = 185$ and $Re_\tau = 395$ were investigated with the adaptive ADM, at two resolutions $N = 31$ and $N = 71$.

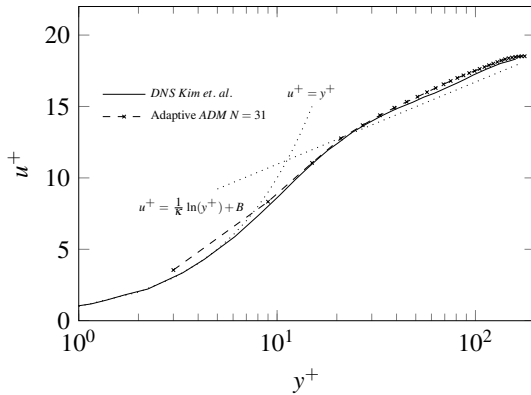


Figure 4: Mean velocity profiles of turbulent channel flow at $Re_\tau = 180$. Comparison of reference DNS of Kim *et al.* (1987) to the underresolved simulations with the BGK-based adaptive ADM model.

In figure 4 the averaged velocity profiles for $Re_\tau = 180$, predicted by the adaptive ADM model is presented and compared to the DNS of Kim *et al.* (1987). The setup with $N = 31$ cells per half-width is underresolved since $\Delta y^+ \approx 6$. Due to the applied bounce-back rule, the first fluid node is at $\Delta y^+ \approx 3$. Nevertheless, the log-law region of the flow was predicted very well and only in vicinity of the wall the velocity was slightly overpredicted. Increasing the resolution to $N = 71$ cells did not influence the results significantly.

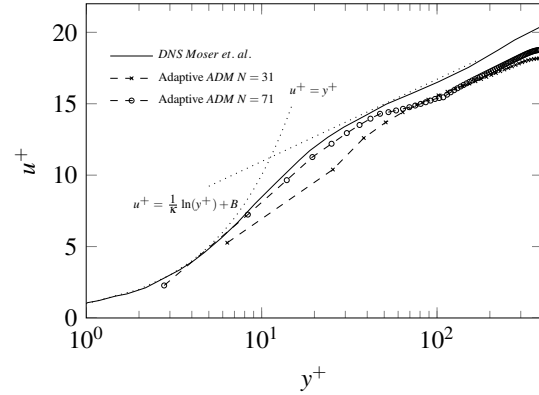


Figure 5: Mean velocity profiles of turbulent channel flow at $Re_\tau = 395$. Comparison of reference DNS of Moser *et al.* (1999) to the underresolved simulations with the BGK-based adaptive ADM model.

In figure 5 the results for $Re_\tau = 395$ when employing the adaptive ADM are shown, for two resolutions of the channel half-width $N = 31$ and $N = 71$, which corresponds to a normalized resolution of $\Delta y^+ \approx 12.8$ and $\Delta y^+ \approx 5.6$ respectively. It is visible, that for the lower resolution $N = 31$ the velocity is generally underpredicted compared to the reference DNS data, while the results for the higher resolution are in good agreement with the DNS for $y^+ < 30$. Although for $N = 71$ the log-law region is slightly underpredicted as well, the adaptive nature of the filtering can be recognized. While the wall nearest region is unaffected by filtering, the scales in the bulk flow are underpredicted and thus, the filter step has an influence on the flow field in the log-law. The bulk flow is underpredicted by both resolutions in the same order of magnitude and it appears, that the constant forcing approach used here is not suitable for the adaptive ADM. Since adaptive filtering is only performed in the log-law region, the damping causes an underprediction of the velocity field, using a constant driving force for the turbulent channel flow. This was also shown for constant filter strengths, see figure 3.

Conclusion

In this paper the lattice Boltzmann method (LBM) was applied to predict turbulent fluid flows. Different collision models were investigated and the single relaxation time scheme was found to be the least dissipative collision model while allowing grid convergence at increasing resolutions. Beyond this it was shown, that the classical approximate deconvolution method (ADM) approach is not suitable for the simulation of wall-bounded flows. This is because the filter strength is chosen quite arbitrary as in Ricot *et al.* (2009) and Ricot *et al.* (2002), and the selective viscosity damping stencils are very dissipative on their own. Thus, a selective filtering approach was presented based on the scales resolved. This approach connects mesh resolution and Reynolds number in terms of a physically motivated energy drain. Although the method is quite dissipative for marginally resolved setups ($N = 31$) at lower Reynolds numbers ($Re_\tau = 180$ and $Re_\tau = 395$), it shows promising results for LES like setups ($N = 71$). Further work is done on dynamic forcing, in order to keep the mass flow constant

and not the absolute volume force. The proposed model is a consistent turbulence model in the framework of the hydrodynamic limit of the filtered Navier-Stokes equations. The explicit filtering step can be extended for complex geometries since a local temporal average is taken into account for the scales resolved.

REFERENCES

- Adams, N. A. & Stolz, S. 2002 A subgrid-scale deconvolution approach for shock capturing. *J. Comp. Phys.* **178**, 391–426.
- Bespalko, D. J. 2011 Validation of the lattice boltzmann method for direct numerical simulation of wall-bounded turbulent flows. dissertation, Queen’s University.
- Chen, S. & Doolen, G. D. 1998 Lattice boltzmann method for fluid flows. *Annu. Rev. Fluid Mech.* **30**, 329–364.
- D’Humières, D., Ginzburg, I., Krafczyk, M., Lallemand, P. & Luo, L.-S. 2002 Multiple-relaxation-time lattice boltzmann models in three dimensions. *Phil. Trans. R. Soc. Lond. A* **361**, 437–451.
- Freitas, R. K., Henze, A., Meinke, M. & Schröder, W. 2011 Analysis of lattice-boltzmann methods for internal flows. *Comp. Fl.* **47**, 115–121.
- Guo, Z., Baochang, S. & Nengchao, W. 2000 Lattice bkg model for incompressible navier stokes equation. *J. Comp. Ph.* **165**, 288–306.
- Guo, Z. & Shu, S. 2013 *Lattice Boltzmann Method and its Applications in Engineering*. World Scientific.
- Hänel, D. 2004 *Molekulare Gasdynamik*. Springer-Verlag.
- He, X. & Luo, L.-S. 1997 Lattice boltzmann model for the incompressible navier stokes equation. *J. Stat. Phys.* **88**, 927–944.
- Jafari, S. & Rahnema, M. 2011 Shear-improved smagorinsky modeling of turbulent channel flow using generalized lattice boltzmann equation. *Int. J. Numer. Meth. Fluids* **67**, 700–712.
- Kim, J., Moin, P. & Moser, R. 1987 Turbulence statistics in fully-developed channel flow at low reynolds-number. *J. Fluid Mech.* **177**, 133–166.
- Lallemand, P. & Luo, L. S. 2000 Theory of the lattice boltzmann method: Dispersion, dissipation, isotropy, galilean invariance, and stability. *Phys. Rev. E* **61**, 6546.
- Latt, J. 2007 Hydrodynamic limit of lattice boltzmann equations. dissertation, Université de Genève.
- Latt, J. & Chopard, B. 2006 Lattice boltzmann method with regularized non-equilibrium distribution functions. *Mathematics and Computer in Simulation* **72**, 165–168.
- Latt, J, Chopard, B., Malaspinas, O., Deville, M. & Michel, A. 2008 Straight velocity boundaries in the lattice boltzmann method. *Phys. Rev. E* **77**, 056703.
- Lèveque, E., Toschi, F., Shao, L. & Bertoglio, J. P. 2007 Shear-improved smagorinsky model for large-eddy simulation of wall-bounded turbulent flows. *J. Fl. Mech.* **570**, 491–502.
- Malaspinas, O. & Sagaut, P. 2011 Advanced large-eddy simulation for lattice boltzmann methods: The approximate deconvolution model. *Phys. Fluids* **23**, 105103.
- Malaspinas, O. & Sagaut, P. 2012 Consistent subgrid scale modelling for lattice boltzmann methods. *J. Fluid Mech.* **700**, 514–542.
- Mathew, J., Lechner, R., Foysi, H., Sesterhenn, J. & Friedrich, R. 2003 An explicit filtering method for large eddy simulation of compressible flows. *Phys. Fluids* **15**, 2279.
- Moser, R. D., Kim, J. & Mansour, N. N. 1999 Direct numerical simulation of turbulent channel flow up to $re_\tau = 590$. *Phys. Fl.* **11**, 943–945.
- Pruett, C. D. & Adams, N. A. 2000 A priori analyses of three subgrid-scale models for one-parameter families of filters. *Phys. Fl.* **12**, 1133–1142.
- Ricot, D., Maillar, V. & Bailly, C. 2002 Numerical simulation of unsteady cavity flow using lattice boltzmann method. In *8th AIAA/CEAS Aeroacoustics Conference & Exhibit*.
- Ricot, D., Marie, S., Sagaut, P. & Bailly, C. 2009 Lattice boltzmann method with selective viscosity filter. *J. Comp. Phys* **228**, 4478–4490.
- Sagaut, P. 2010 Toward advanced subgrid models for lattice-boltzmann-based large-eddy simulation: Theoretical formulations. *Computers and Mathematics with Applications* **59**, 2194–2199.
- Stolz, S. & Adams, N. A. 1999 An approximate deconvolution procedure for large-eddy simulation. *Phys. Fluids* **11**, 1699.
- Stolz, S., Adams, N. A. & Kleiser, L. 2001 An approximate deconvolution model for large-eddy simulation with application to incompressible wall-bounded flows. *Phys. Fluids* **13**, 997.
- Sukop, M. C. & Thorne, D. T. 2006 *Lattice Boltzmann Modeling*. Springer-Verlag.
- Tam, C. K. W., C., Webb J. & Dong, Zhong 1993 A study of the short wave components in computational acoustics. *J. Comp. Acous.* **1**, 133–166.
- Waldrow, D. A. 2000 *Lattice-Gas Cellular Automata and Lattice Boltzmann Models: An Introduction*. Springer-Verlag.